12 - volume growth
skin expansion & growth

Journal of the Mechanics and Physics of Solids 59 (2011) 2177–2190
Contents lists available at ScienceDirect
Journal of the Mechanics and Physics of Solids
journal homepage: www.elsevier.com/locate/jmps

Growing skin: A computational model for skin expansion in reconstructive surgery

Adrián Buganza Tepole [a], Christopher Joseph Ploch [a], Jonathan Wong [a], Arun K. Gosain [b], Ellen Kuhl [a,c,d,*]

[a] Department of Mechanical Engineering, Stanford University, Stanford, CA 94305, USA
[b] Department of Plastic Surgery, Rainbow Babies and Children's Hospital, Case Western Reserve University, Cleveland, OH 44106, USA
[c] Department of Bioengineering, Stanford University, Stanford, CA 94305, USA
[d] Department of Cardiothoracic Surgery, Stanford University, Stanford, CA 94305, USA

ARTICLE INFO

Article history:
Received 15 February 2011
Received in revised form
5 May 2011
Accepted 14 May 2011
Available online 24 May 2011

Keywords:
Growth
Finite element modeling
Skin
Tissue expansion
Reconstructive surgery

ABSTRACT

The goal of this manuscript is to establish a novel computational model for stretch-induced skin growth during tissue expansion. Tissue expansion is a common surgical procedure to grow extra skin for reconstructing birth defects, burn injuries, or cancerous breasts. To model skin growth within the framework of nonlinear continuum mechanics, we adopt the multiplicative decomposition of the deformation gradient into an elastic and a growth part. Within this concept, we characterize growth as an irreversible, stretch-driven, transversely isotropic process parameterized in terms of a single scalar-valued growth multiplier, the in-plane area growth. To discretize its evolution in time, we apply an unconditionally stable, implicit Euler backward scheme. To discretize it in space, we utilize the finite element method. For maximum algorithmic efficiency and optimal convergence, we suggest an inner Newton iteration to locally update the growth multiplier at each integration point. This iteration is embedded within an outer Newton iteration to globally update the deformation at each finite element node. To demonstrate the characteristic features of skin growth, we simulate the process of gradual tissue expander inflation. To visualize growth-induced residual stresses, we simulate a subsequent tissue expander deflation. In particular, we compare the spatio-temporal evolution of area growth, elastic strains, and residual stresses for four commonly available tissue expander geometries. We believe that predictive computational modeling can open new avenues in reconstructive surgery to rationalize and standardize clinical process parameters such as expander geometry, expander size, expander placement, and inflation timing.

International Journal of Non-Linear Mechanics 47 (2012) 938–949
Contents lists available at ScienceDirect
International Journal of Non-Linear Mechanics
journal homepage: www.elsevier.com/locate/nlm

Stretching skin: The physiological limit and beyond ☆

Adrián Buganza Tepole [a], Arun K. Gosain [b], Ellen Kuhl [c,*]

[a] Department of Mechanical Engineering, Stanford University, Stanford, CA 94305, USA
[b] Department of Plastic Surgery, Rainbow Babies and Children's Hospital, Case Western Reserve University, Cleveland, OH 44106, USA
[c] Departments of Mechanical Engineering, Bioengineering, and Cardiothoracic Surgery, Stanford University, Stanford, CA 94305, USA

ARTICLE INFO

Available online 23 July 2011

Keywords:
Skin
Growth
Wormlike chain model
Chain network model
Finite element modeling
Tissue expansion

ABSTRACT

The goal of this paper is to establish a novel computational model for skin to characterize its constitutive behavior when stretched within and beyond its physiological limits. Within the physiological regime, skin displays a reversible, highly non-linear, stretch locking, and anisotropic behavior. We model these characteristics using a transversely isotropic chain network model composed of eight wormlike chains. Beyond the physiological limit, skin undergoes an irreversible area growth triggered through mechanical stretch. We model skin growth as a transversely isotropic process characterized through a single internal variable, the scalar-valued growth multiplier. To discretize the evolution of growth in time, we apply an unconditionally stable, implicit Euler backward scheme. To discretize it in space, we utilize the finite element method. For maximum algorithmic efficiency and optimal convergence, we suggest an inner Newton iteration to locally update the growth multiplier at each integration point. This iteration is embedded within an outer Newton iteration to globally update the deformation at each finite element node. To illustrate the characteristic features of skin growth, we first compare the two simple model problems of displacement- and force-driven growth. Then, we model the process of stretch-induced skin growth during tissue expansion. In particular, we compare the spatio-temporal evolution of stress, strain, and area gain for four commonly available tissue expander geometries. We believe that the proposed model has the potential to open new avenues in reconstructive surgery and rationalize critical process parameters in tissue expansion, such as expander geometry, expander size, expander placement, and inflation timing.

Biomech Model Mechanobiol (2012) 11:855–867
DOI 10.1007/s10237-011-0357-4
ORIGINAL PAPER

Growing skin: tissue expansion in pediatric forehead reconstruction

Alexander M. Zöllner · Adrian Buganza Tepole · Arun K. Gosain · Ellen Kuhl

Received: 29 July 2011 / Accepted: 20 October 2011 / Published online: 4 November 2011

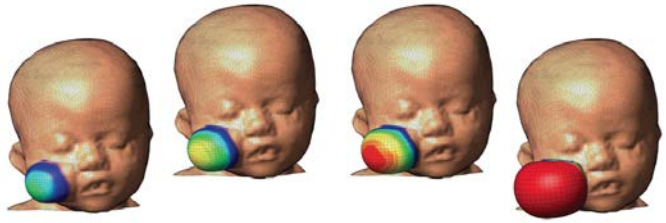

Journal of Theoretical Biology 297 (2012) 166–175

Contents lists available at SciVerse ScienceDirect

Journal of Theoretical Biology

journal homepage: www.elsevier.com/locate/yjtbi

On the biomechanics and mechanobiology of growing skin

Alexander M. Zöllner [a], Adrian Buganza Tepole [a], Ellen Kuhl [a,b,c,d,*]

[a] Department of Mechanical Engineering, Stanford University, Stanford, CA 94305, USA
[b] Department of Mechanical and Process Engineering, Center of Mechanics, ETH Zurich, 8092 Zurich, Switzerland
[c] Department of Bioengineering, Stanford University, Stanford, CA 94305, USA
[d] Department of Cardiothoracic Surgery, Stanford University, Stanford, CA 94305, USA

ARTICLE INFO

Article history:
Received 29 October 2011
Received in revised form
6 December 2011
Accepted 21 December 2011
Available online 4 January 2012

Keywords:
Skin
Biological membranes
Mechanotransduction
Growth
Tissue expansion

ABSTRACT

Skin displays an impressive functional plasticity, which allows it to adapt gradually to environmental changes. Tissue expansion takes advantage of this adaptation, and induces a controlled in situ skin growth for defect correction in plastic and reconstructive surgery. Stretches beyond the skin's physiological limit invoke several mechanotransduction pathways, which increase mitotic activity and collagen synthesis, ultimately resulting in a net gain in skin surface area. However, the interplay between mechanics and biology during tissue expansion remains unquantified. Here, we present a continuum model for skin growth that summarizes the underlying mechanotransduction pathways collectively in a single phenomenological variable, the strain-driven area growth. We illustrate the governing equations for growing biological membranes, and demonstrate their computational solution within a nonlinear finite element setting. In displacement-controlled equi-biaxial extension tests, the model accurately predicts the experimentally observed histological, mechanical, and structural features of growing skin, both qualitatively and quantitatively. Acute and chronic elastic uniaxial stretches are 25% and 10%, compared to 36% and 10% reported in the literature. Acute and chronic thickness changes are −28% and −12%, compared to −22% and −7% reported in the literature. Chronic fractional weight gain is 3.3, compared to 2.7 for wet weight and 3.3 for dry weight reported in the literature. In two clinical cases of skin expansion in pediatric forehead reconstruction, the model captures the clinically observed mechanical and structural responses, both acutely and chronically. Our results demonstrate that the field theories of continuum mechanics can reliably predict the mechanical manipulation of thin biological membranes by controlling their mechanotransduction pathways through mechanical over-stretch. We anticipate that the proposed skin growth model can be generalized to arbitrary biological membranes, and that it can serve as a valuable tool to virtually manipulate living tissues, simply by means of changes in the mechanical environment.

© 2011 Elsevier Ltd. All rights reserved.

motivation – class project 2010 5

skin is a multi-layered material

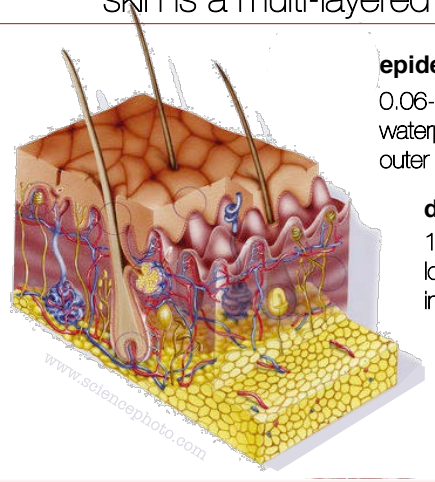

epidermis
0.06-1.0mm thick
waterproof, protective
outer layer

dermis
1.0-3.0mm thick
load bearing
inner layer

hypodermis
fatty layer
attaching skin
to bone and muscle

motivation - skin growth 6

skin expansion

`skin expansion` is a technique used by plastic and restorative surgeons to cause the body grow additional skin. keeping living tissues under tension causes new cells to form and the amount of tissue to increase. in some cases, this may be accomplished by the implantation of inflatable balloons under the skin. by far the most common method, the surgeon inserts the inflatable expander beneath the skin and periodically, over weeks or months, injects a saline solution to slowly stretch the overlying skin. the growth of tissue is permanent, but will retract to some degree when the expander is removed. within the past 30 years, skin expansion has revolutionized reconstructive surgery. typical applications are breast reconstruction, burn injuries, and pediatric plastic surgery.

WIKIPEDIA
The Free Encyclopedia

motivation - skin growth 7

skin expanders

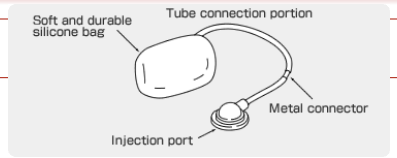

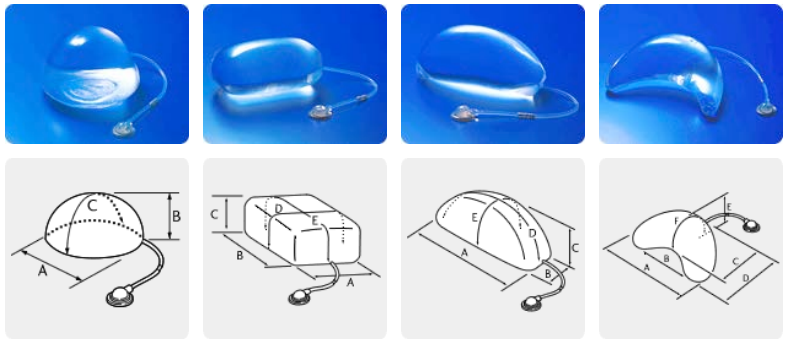

motivation - skin growth 8

mechanotransduction of growing skin

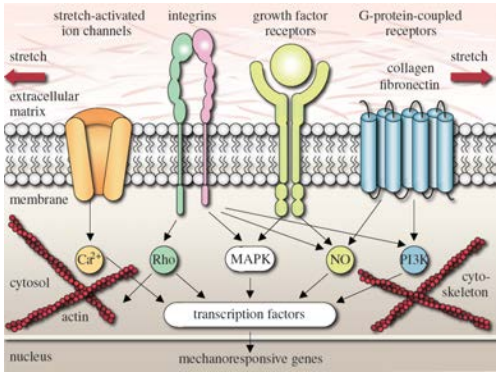

transmembrane mechanosensors in the form of stretch-activated ion channels, integrins, growth factor receptors, and G-protein-coupled receptors translate extracellular signals into intracellular events, which activate a cascade of interconnected signaling pathways. biomechanical and biochemical signals converge in the activation of transcription factors, activating gene expression. mechanotransduction triggers increased mitotic activity and increased collagen synthesis, resulting in an increase in skin surface area to restore the homeostatic equilibrium state. wong et al. [2011], zollner et al. [2011]

langer's lines - anisotropy of human skin

langer's lines, sometimes called cleavage lines, are topological lines drawn on a map of the human body. they are defined by the direction in which the human skin would split when struck with a spike. langer's lines correspond to the natural orientation of collagen fibers in the dermis and epidermis. knowing the direction of langer's lines within a specific area of the skin is important for surgical procedures. particularly cosmetic surgery involving the skin. if a surgeon has a choice about where and in what direction to place an incision, he may choose to cut in the direction of langer's lines. incisions made parallel to langer's lines may heal better and produce less scarring than those cut across.

langer's lines - anisotropy of human skin

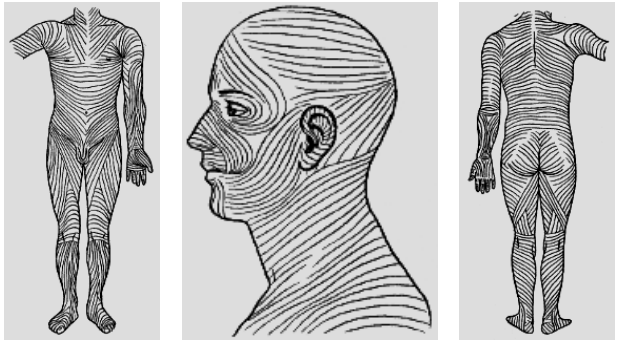

lines of tension - orientation of collagen fiber bundles

carl ritter von langer [1819-1887]

langer's lines - anisotropy of rabbit skin

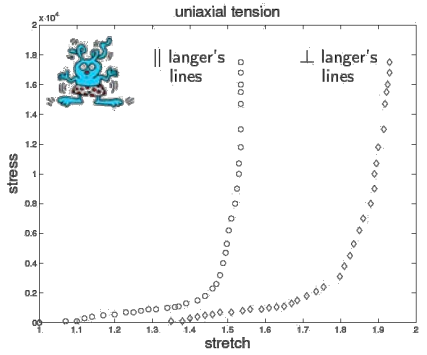

stiffer || to langer's lines - stress locking @crit stretch

lanir & fung [1974]

what is it that makes skin anisotropic? collagen fibers

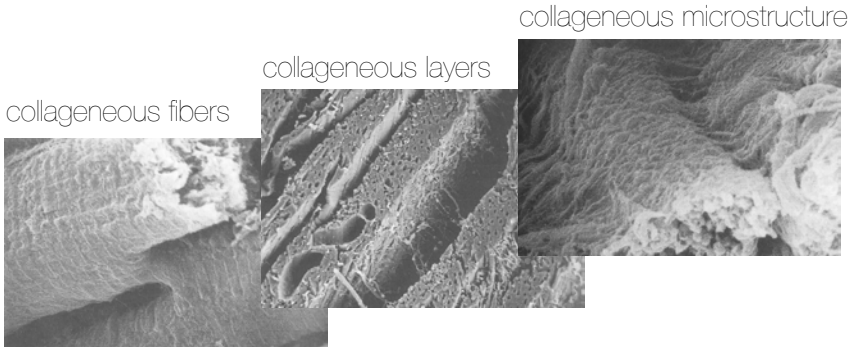

directional strengthening due to collagen fibers

humphrey [2002]

collagen fibers - hierarchical microstructure

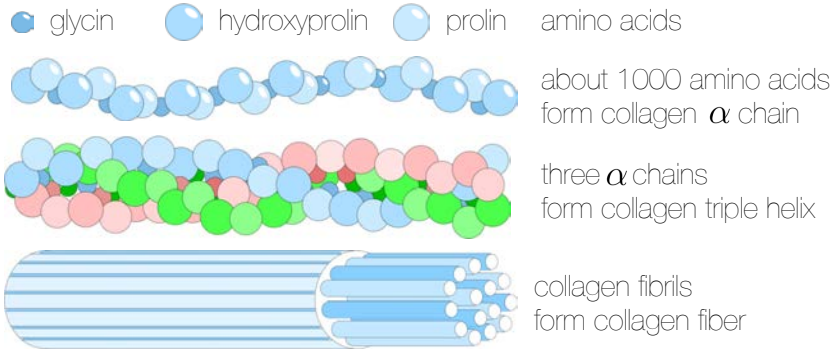

directional strengthening due to collagen fibers

statistical mechanics of long chain molecules

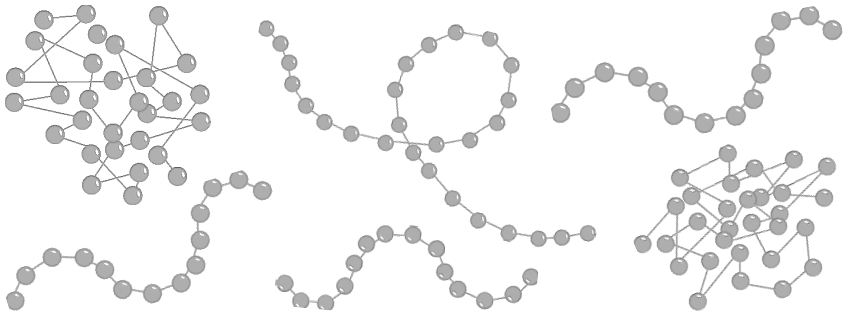

entropic elasticity - entropy increases upon stretching

kuhn [1936], [1938], porod [1949], kratky & porod [1949], treolar [1958], flory [1969], bustamante, smith, marko & siggia [1994], marko & siggia [1995], rief [1997], holzapfel [2000], bischoff, arruda & grosh [2000], [2002], ogden, saccomandi & sgura [2006]

uncorrelated chain model - freely jointed chain

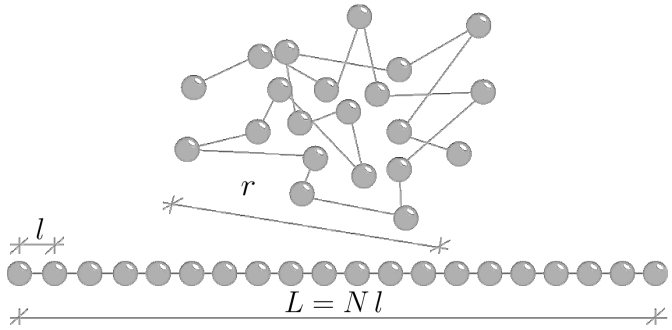

$$\psi^{\text{fjc}} = k\,\theta\,N\left[\frac{r}{L}\mathcal{L}^{-1} + \ln\left(\frac{\mathcal{L}^{-1}}{\sinh(\mathcal{L}^{-1})}\right)\right]$$

micromechanically motivated parameter - contour length L

correlated chain model - wormlike chain

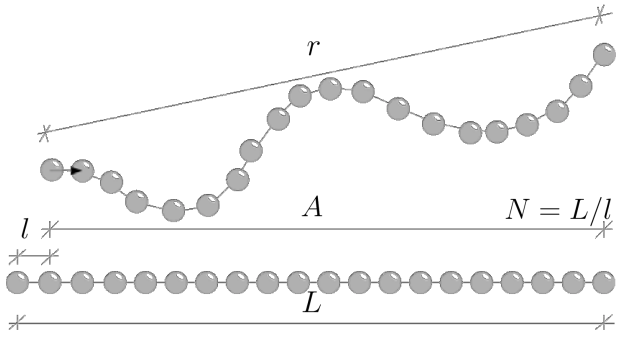

$$\psi^{\mathrm{wlc}} = \frac{k\,\theta\,\boldsymbol{L}}{4\,\boldsymbol{A}}\left[2\,\frac{r^2}{\boldsymbol{L}^2} + \frac{1}{[1-r/\boldsymbol{L}]} - \frac{r}{\boldsymbol{L}}\right]$$

micromechanically motivated parameters - contour length $\boldsymbol{L}$ and persistence length $\boldsymbol{A}$

uncorrelated vs correlated chain model

$$f^{\mathrm{fjc}} = k\,\theta\,N\mathcal{L}^{-1}(\tfrac{r}{L}) \qquad f^{\mathrm{wlc}} = \tfrac{k\,\theta}{4\,A}\left[\tfrac{4\,r}{L} + \tfrac{1}{[1-r/L]^2} - 1\right]$$

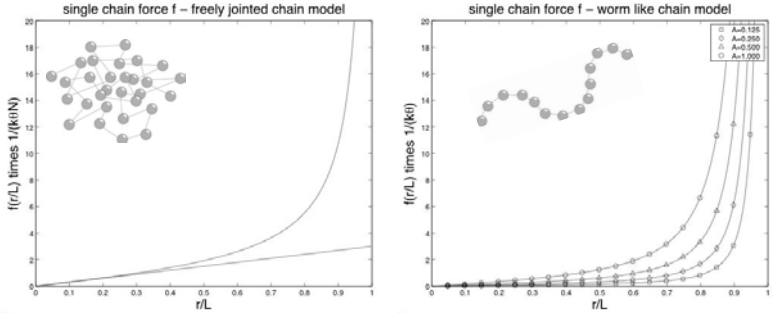

characteristic locking behavior - initial stiffness of wlc

micromechanically motivated parameters - contour length $\boldsymbol{L}$ and persistence length $\boldsymbol{A}$

chain network models

three chain model | four chain model | eight chain model

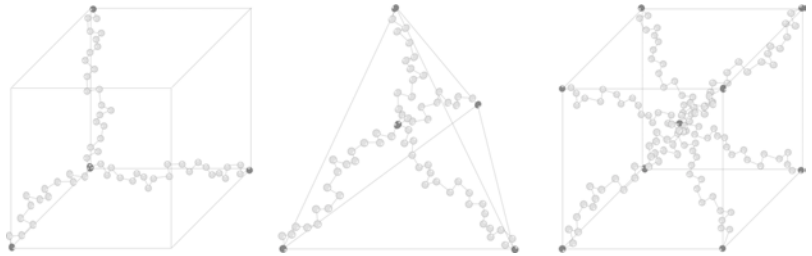

representative isotropic network of cross-linked chains

flory & rehner [1943], james & guth [1943], wang & guth [1952], treloar [1958], arruda & boyce [1993], wu & van der giessen [1993], boyce [1996], boyce & arruda [2000], bischoff, arruda & grosh [2002], miehe, göktepe & lulei [2004]

generalized eight chain model

eight single chains | isotropic cell matrix | eight chain model

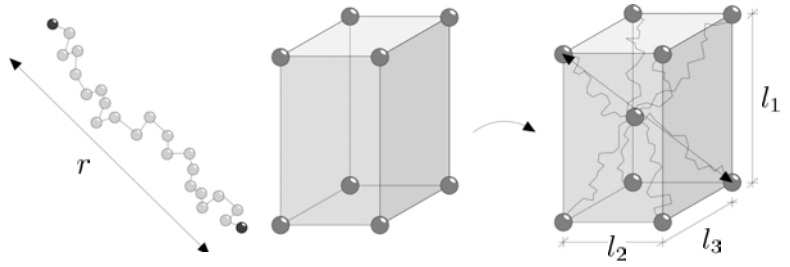

$$\Psi^{\mathrm{chn}} = \tfrac{1}{8}\,\gamma^{\mathrm{chn}}\textstyle\sum_{i=1}^{8}\psi^{\mathrm{wlc}}(r) \qquad \text{with} \qquad r = r(\boldsymbol{F})$$

$$\Psi^{\mathrm{iso}} = \tfrac{1}{2}\,\lambda\ln^2(\det(\boldsymbol{F})) + \tfrac{1}{2}\,\mu[\,\boldsymbol{F}^{\mathrm{t}} : \boldsymbol{F} - n^{\mathrm{dim}} - 2\,\ln(\det(\boldsymbol{F}))\,]$$

micromechanically motivated parameters - chain density γ^{chn} and cell dimensions l_1, l_2, l_3

generalized eight chain model

- general case orthotropic network model

$l_1 \neq l_2 \neq l_3 \qquad r = \sqrt{l_I^2\, \bar{I}_I^C}$

- special case isotropic network model

$l_1 = l_2 = l_3 = l \qquad r = l\sqrt{I_1^C}$

- special case transversely isotropic model

$l_2 = l_3 = 0 \qquad r = l_1\sqrt{\bar{I}_1^C}$

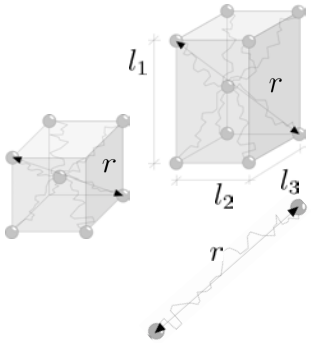

traditional arruda boyce model as special case

invariants $I_1^C = \boldsymbol{C} : \boldsymbol{I}$ and $\bar{I}_I^C = \boldsymbol{n}_I \cdot \boldsymbol{C} \cdot \boldsymbol{n}_I$

experiment vs simulation - rabbit skin

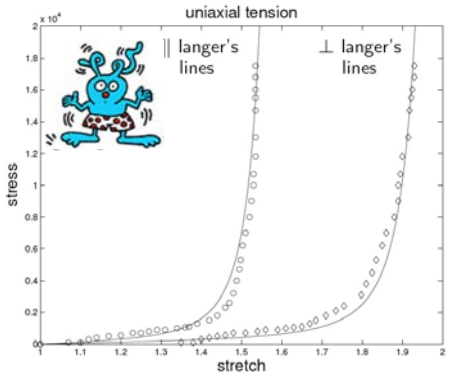

stiffer || to langer's lines - stress locking @crit stretch

lanir & fung [1974], kuhl, garikipati, arruda & grosh [2005]

sometimes skin is damaged…

congenital nevomelanocytic nevi, pigmented surface lesions, are present in one per cent of newborns. one in 20,000 newborns is born with a giant congenital nevus, larger than 10cm in diameter. congenital nevi need to be removed, usually about 6 months after birth, not only because of their cosmetic appearance, but also because of their high potential for malignant change.

… but we can repair it

partial reconstruction of right ear. fig 1. preoperative status of partial traumatic amputation of right ear. fig 2. a rubber balloon is inserted in the subcutaneous tissue. fig 3. the rubber balloon is inflated gradually over a period of six weeks. fig 4. upon removal of the balloon, a c-shaped autogenous graft was introduced and covered by a double pedicled tubed flap fashioned from the skin expanded by balloon inflation. neumann [1957]

skin expansion and growth - breast reconstruction

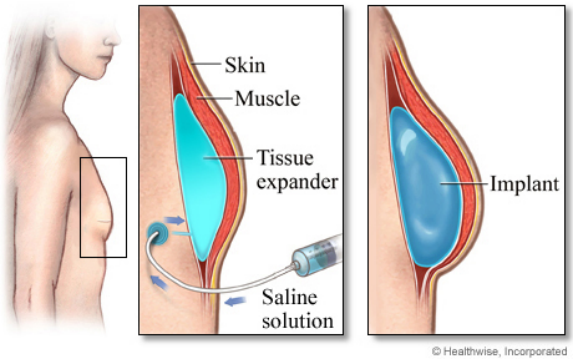

within the past 30 years, tissue expansion has revolutionized reconstrutive surgery. typical application are breast reconstruction, burn injuries, and pediatric plastic surgery. natural tissue expansion can be observed in pregnancy, where the local tissue expands and growth in area in response to tension.

skin expansion and growth - facial reconstruction

eight-year-old boy who had a nevus removed as an infant. tissue expansion is completed in approximately ten weeks. the use of tissue expansion in cosmetic precedures is often limited by the significant deformity the patient must temporarily accept during the four to six week long procedure.

mangubat [2010]

skin expansion and growth - facial reconstruction

in this study of reconstruction of the forehead in children, the average number of surgical procedures required to complete reconstruction was six, involving an average of three tissue expansion proecures.

gosain & cortes [2007]

skin expansion and growth - ear gauging

there are many different methods you can choose from to stretch your ears. always wait at least one month between stretching. failure to stick to this could result in your earlobe puckering, being very thin, or even tearing completely apart. **tapering** is the most common way to stretch ears today. it involves the use of a taper, a rod that is larger at one end, specifically made for this purpose. the taper is lubricated and pushed though the hole until the larger end is flush with the earlobe. rings are then pushed though, parallel to the end of the taper. no equipment is used **dead stretching**. larger jewelry is just forced though the existing piercing. large **weights** can be used to stretch the piercing.

skin expansion and growth - lip plates

among the surma and mursi in ethiopia, about 6 to 12 months before marriage the woman's lip is pierced, usually at around the age of 15 to 18. the initial piercing is done as an incision of the lower lip of 1 to 2 cm length, and a simple wooden peg is inserted. after the wound has healed, which usually takes 2 or 3 weeks, the peg is replaced with a slightly bigger one. at a diameter of about 4 cm the first lip plate made of clay is inserted. every woman crafts her plate by herself and takes pride in including some ornamentation. the final diameter ranges from about 8 cm to over 20 cm. the plate's size is a sign of social or economical importance in some tribes.

http://www.mursi.org

schematic sequence of tissue expansion

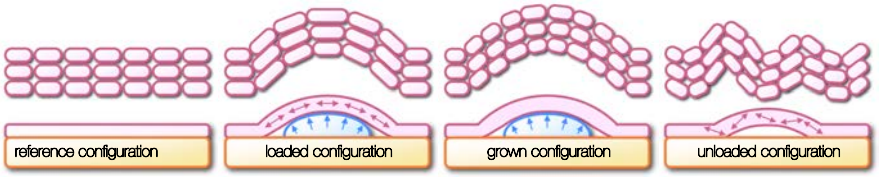

at biological equilibrium, the skin is in a physiological state of resting tension. a tissue expander is implanted subcutaneously between the skin and the hypodermis. when the expander is inflated, mechanical stretch induces cell proliferation causing the skin to grow. growth restores the state of resting tension. expander deflation reveals residual stresses in the skin layer.

kinematics of finite growth

$$\boldsymbol{F} = \boldsymbol{F}_{\mathrm{e}} \cdot \boldsymbol{F}_{\mathrm{g}}$$

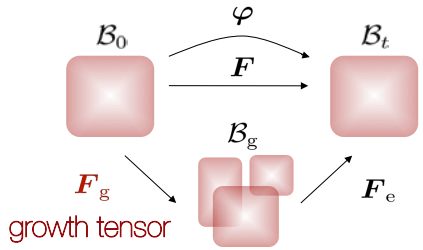

multiplicative decomposition

lee [1969], simo [1992], rodriguez, hoger & mc culloch [1994], epstein & maugin [2000], humphrey [2002], ambrosi & mollica [2002], himpel, kuhl, menzel & steinmann [2005]

kinematics of finite growth

$$\boldsymbol{F} = \boldsymbol{F}_\mathrm{l} \cdot \boldsymbol{F}_\mathrm{c} \cdot \boldsymbol{F}_\mathrm{g}$$

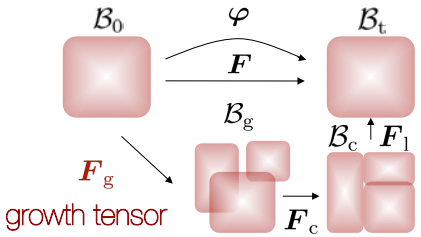

growth tensor

$\boldsymbol{F}_\mathrm{e} = \boldsymbol{F}_\mathrm{l} \cdot \boldsymbol{F}_\mathrm{c}$

compatibility tensor

multiplicative decomposition

lee [1969], simo [1992], rodriguez, hoger & mc culloch [1994], epstein & maugin [2000], humphrey [2002], ambrosi & mollica [2002], himpel, kuhl, menzel & steinmann [2005]

kinematic equations

kinematics of finite growth

$$\boldsymbol{F} = \boldsymbol{F}_\mathrm{l} \cdot \boldsymbol{F}_\mathrm{c} \cdot \boldsymbol{F}_\mathrm{g}$$

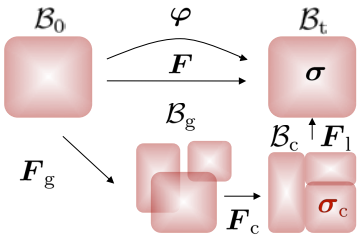

total stress

residual stress

residual stress

the additional deformation of squeezing the grown parts back to a compatible configuration gives rise to residual stresses (see thermal stresses)

kinematic equations

skin expansion and growth

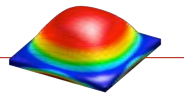

$$\boldsymbol{F} = \boldsymbol{F}_\mathrm{l} \cdot \boldsymbol{F}_\mathrm{c} \cdot \boldsymbol{F}_\mathrm{g}$$

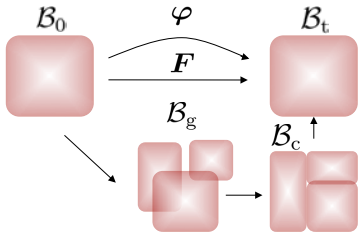

growth tensor

$$\boldsymbol{F}_\mathrm{g} = \begin{bmatrix} \lambda_\mathrm{m}^\mathrm{g} & 0 & 0 \\ 0 & \lambda_\mathrm{p}^\mathrm{g} & 0 \\ 0 & 0 & \lambda_h^\mathrm{g} \end{bmatrix}$$

elastic tensor

$$\boldsymbol{F}_\mathrm{l} = \begin{bmatrix} \lambda_\mathrm{m}^\ell & 0 & 0 \\ 0 & \lambda_\mathrm{p}^\ell & 0 \\ 0 & 0 & \lambda_h^\ell \end{bmatrix}$$

compatibility restoring tensor

$$\boldsymbol{F}_\mathrm{c} = \begin{bmatrix} \lambda_\mathrm{m}^{\mathrm{eg}} & 0 & 0 \\ 0 & \lambda_\mathrm{p}^{\mathrm{eg}} & 0 \\ 0 & 0 & \lambda_h^{\mathrm{eg}} \end{bmatrix}$$

socci, pennati, gervaso, vena [2007]

example - skin expansion

skin expansion and growth

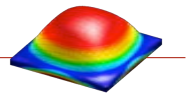

- growth law $\dot{\mathbf{F}}^\mathrm{g} = \dot{\mathbf{U}}^\mathrm{g} = k_\lambda \begin{bmatrix} \lambda_\mathrm{m}^\ell - 1 & 0 & 0 \\ 0 & \lambda_\mathrm{p}^\ell - 1 & 0 \\ 0 & 0 & 0 \end{bmatrix}$
- increase in mass $\dot{m} = \delta \int_V \mathrm{div}(\mathbf{v}^\mathrm{g})\mathrm{d}V = \delta \int_V (D_{11}^\mathrm{g} + D_{22}^\mathrm{g} + D_{33}^\mathrm{g})\mathrm{d}V$
- rate of growth deformation tensor $\mathbf{D}^\mathrm{g} = \frac{1}{2}\left[\dot{\mathbf{U}}^\mathrm{g}(\mathbf{U}^\mathrm{g})^{-1} + (\mathbf{U}^\mathrm{g})^{-1}\dot{\mathbf{U}}^\mathrm{g}\right]$
- rate of mass increase $\dot{m} = \delta k_\lambda \int_V \left[\frac{(\lambda_\mathrm{m}^\mathrm{l} - 1)}{\lambda_\mathrm{m}^\mathrm{g}} + \frac{\left(\lambda_\mathrm{p}^\mathrm{l} - 1\right)}{\lambda_\mathrm{p}^\mathrm{g}}\right]\mathrm{d}V$

socci, pennati, gervaso, vena [2007]

example - skin expansion

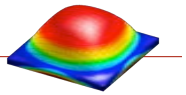

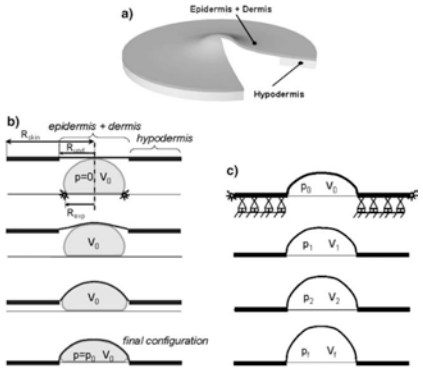

Fig 2. 2a. Sketch of model of expanded skin showing the two considered layers. 2b. First step of simulation of skin expansion: thee successive phases of skin-expander interaction. 2c. Second step of simulation of skin expansion: three successive phases of skin-expander model.

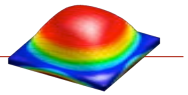

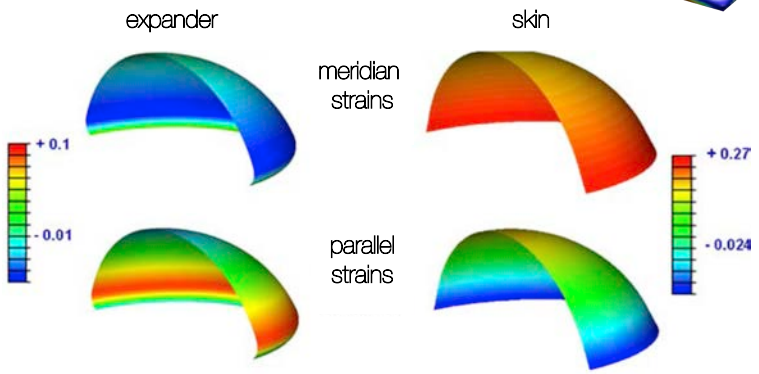

Fig 7. Contour plot of logarithmic principal strains for expander (left) and skin (right) at volume of 550 ml.

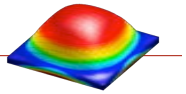

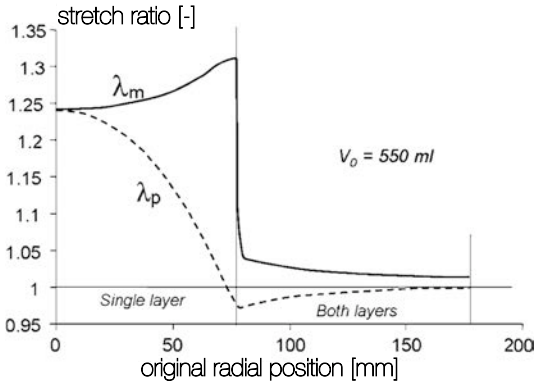

Fig 8. Meridian and parallel stretch ratios vs. distance from the axis of symmetry of the two skin regions (single layer and two layers) after expander injection at reference volume V_0.

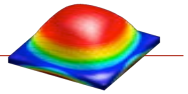

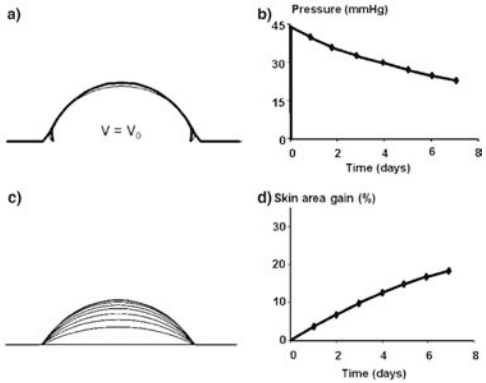

Fig 10. Results of skin growth simulation. 10a. Configurations of expander and expander skin immediately after inflation (thin line) and one week post inflation (thick line). 10b. Pressure decrease during one week after inflation. 10c. Different stress-free configurations at times d0 to d7 at increments of one day. 10d. Percentage of skin area gain.

stretch-induced area growth

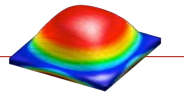

- deformation gradient

$$\boldsymbol{F} = \boldsymbol{F}^{\mathrm{e}} \cdot \boldsymbol{F}^{\mathrm{g}} \quad \text{with} \quad \boldsymbol{F} = \nabla_X \boldsymbol{\varphi}$$

- volume change

$$J = J^{\mathrm{e}}\, J^{\mathrm{g}} \quad \text{with} \quad J = \det(\boldsymbol{F}) > 0$$

- area change

$$\vartheta = \vartheta^{\mathrm{e}}\, \vartheta^{\mathrm{g}} \quad \text{with} \quad \vartheta = \| \operatorname{cof}(\boldsymbol{F}) \cdot \boldsymbol{n}_0 \|$$

- growth tensor

$$\boldsymbol{F}^{\mathrm{g}} = \sqrt{\vartheta^{\mathrm{g}}}\, \boldsymbol{I} + [\, 1 - \sqrt{\vartheta^{\mathrm{g}}}\,]\, \boldsymbol{n}_0 \otimes \boldsymbol{n}_0$$

goriely, ben amar [2005], ben amar, goriely [2005,2007], socci, rennati, geraso, vena [2007], dervaux, ciarletta, ben amar [2009], goktepe, abilez, kuhl [2010], mc mahon, goriely [2010], buganza tepole, ploch, wong, gosain, kuhl [2011], buganza tepole, gosain, kuhl [2011], li, cao, feng, gao [2011]

stretch-induced area growth

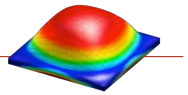

- growth tensor

$$\boldsymbol{F}^{\mathrm{g}} = \sqrt{\vartheta^{\mathrm{g}}}\, \boldsymbol{I} + [\, 1 - \sqrt{\vartheta^{\mathrm{g}}}\,]\, \boldsymbol{n}_0 \otimes \boldsymbol{n}_0$$

- area growth

$$\dot{\vartheta}^{\mathrm{g}} = k^{\mathrm{g}}(\vartheta^{\mathrm{g}})\, \phi^{\mathrm{g}}(\vartheta^{\mathrm{e}})$$

- weighting function

$$k^{\mathrm{g}} = [[\vartheta^{\max} - \vartheta^{\mathrm{g}}]/[\vartheta^{\max} - 1]]^{\gamma}/\tau$$

- growth criterion

$$\phi^{\mathrm{g}} = \vartheta^{\mathrm{e}} - \vartheta^{\mathrm{crit}} = \vartheta/\vartheta^{\mathrm{g}} - \vartheta^{\mathrm{crit}}$$

himpel, kuhl, menzel, steinmann [2005], kuhl, maas, himpel, menzel [2007], goktepe, abilez, parker, kuhl [2010], goktepe, abilez, kuhl [2010], schmid, pauli, paulus, kuhl [2011], buganza tepole, ploch, wong, gosain, kuhl [2011], buganza tepole, gosain, kuhl [2011]

time integration - euler backward

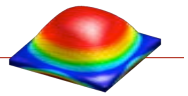

- finite difference approximation

$$\dot{\vartheta}^{\mathrm{g}} = \frac{1}{\Delta t}\, [\, \vartheta^{\mathrm{g}} - \vartheta^{\mathrm{g}}_{\mathrm{n}}\,] = k^{\mathrm{g}}(\vartheta^{\mathrm{g}})\, \phi^{\mathrm{g}}(\vartheta^{\mathrm{e}})$$

- residual of discrete evolution equation

$$\mathrm{R}^{\mathrm{g}} = \vartheta^{\mathrm{g}} - \vartheta^{\mathrm{g}}_{\mathrm{n}} - k^{\mathrm{g}}\, \phi^{\mathrm{g}}\, \Delta t \doteq 0$$

- linearized residual for local newton iteration

$$\mathrm{K}^{\mathrm{g}} = \frac{\partial \mathrm{R}^{\mathrm{g}}}{\partial \vartheta^{\mathrm{g}}} = 1 - \left[\frac{\partial k^{\mathrm{g}}}{\partial \vartheta^{\mathrm{g}}}\, \phi^{\mathrm{g}} + k^{\mathrm{g}}\, \frac{\partial \phi^{\mathrm{g}}}{\partial \vartheta^{\mathrm{g}}} \right] \Delta t$$

- iterative update of growth multiplier

$$\vartheta^{\mathrm{g}} \leftarrow \vartheta^{\mathrm{g}} - \mathrm{R} \,/\, \mathrm{K}$$

the adrian me337-model [2010]

relaxation & creep

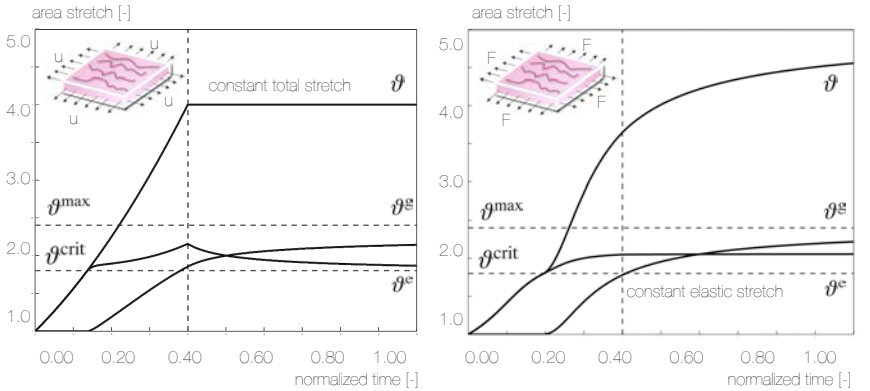

temporal evolution of total area stretch, reversible elastic area stretch, and irreversible growth area stretch for displacement- and force-controlled skin expansion. displacement control induces relaxation, a decrease in elastic stretch, while the growth stretch increases at a constant total stretch. force control induces creep, a gradual increase in growth stretch and total stretch at constant elastic stretch.

current gold standard in expander selection

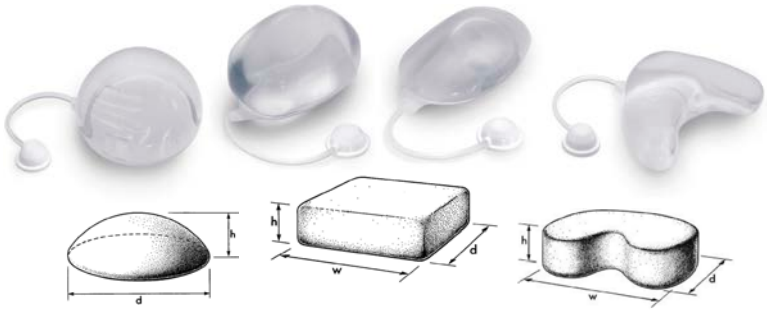

$A_{growth} = A_t - A_0 = 2h\,[w+d]$

empirical correction factors: 6.00, 3.75, and 4.50

van rappard, molenaar, van doorn, sonneveld, borghouts [1988]
shively [1986], duits, molenaar, van rappard [1989]

example - skin expansion

predictive modeling for expander selection

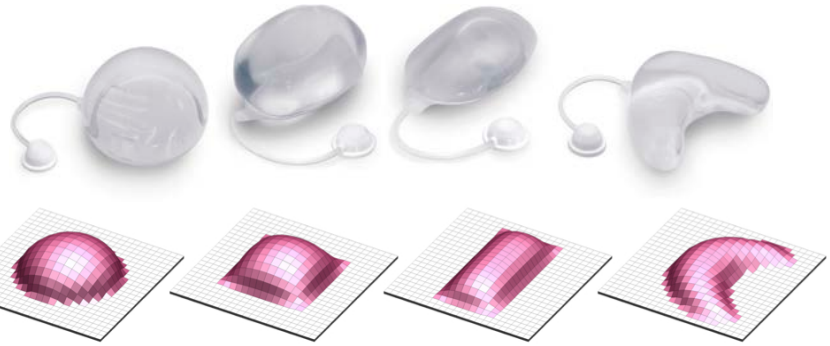

skin is modeled as a 0.2cm thin 12'12cm2 square sheet, discretized with 3'24'24=1728 trilinear brick elements, with 4'25'25=2500 nodes and 7500 degrees of freedom. the base surface area of all expanders is scaled to 148 elements corresponding to 37cm2. this area, shown in red, is gradually pressurized from below while the bottom nodes of all remaining elements, shown in white, are fixed.

example - skin expansion

fractional area gain & expander volume

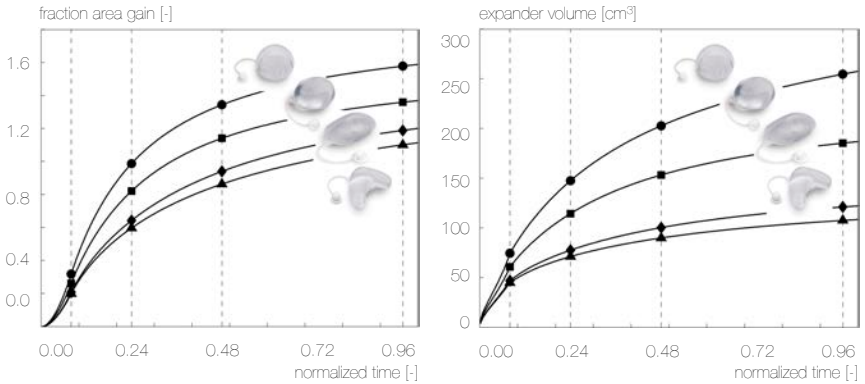

tissue expander inflation. expanders are inflated gradually between t=0.00 and t=0.08 by linearly increasing the pressure, which is then held constant from t=0.08 to t=1.00 to allow the skin to grow. under the same pressure, the circular expander displays the largest fractional area gain and expander volume, followed by the square, the rectangular, and the crescent-shaped expanders.

example - skin expansion

quantitative expander selection

	maximum growth ϑ^g [-]	initial area A_0 [cm²]	absolute area gain ΔA [cm²]	fractional area gain $\Delta A/A_0$ [-]	expander volume V [cm³]	expander pressure p/E [-]	residual stress σ^{max} /E [-]
circular	2.36	37.00	58.74	1.59	257.45	0.002	0.42
square	2.35	37.00	50.63	1.37	186.77	0.002	0.41
rectangular	2.26	37.00	44.40	1.20	122.06	0.002	0.34
crescent	2.25	37.00	41.19	1.11	108.42	0.002	0.33

tissue expander inflation and deflation. maximum growth multiplier, absolute area gain, fractional area gain, and expander volume under constant pressure loading at time t=50 and maximum principal residual stresses upon unloading after a constant pressure growth until t=12 are are largest for the circular expander, followed by the square, the rectangular, and the crescent shape expanders.

example - skin expansion

area growth - isotropic skin model

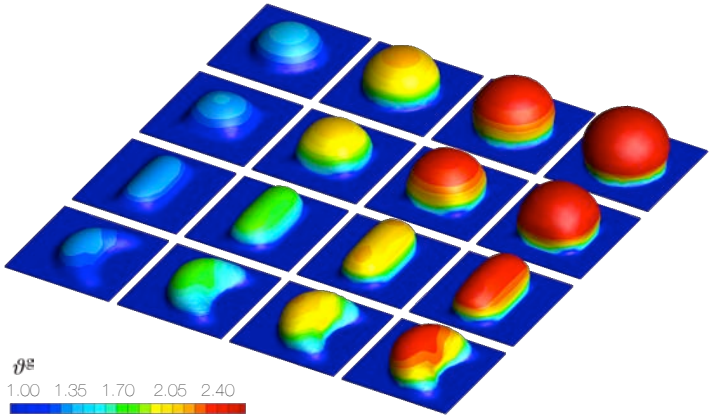

tissue expander inflation. spatio-temporal evolution of area growth. under the same pressure applied to the same base surface area, the circular expander induces the largest amount of growth followed by the square, the rectangular, and the crescent-shaped expanders.

example - skin expansion 49

elastic stretch - isotropic skin model

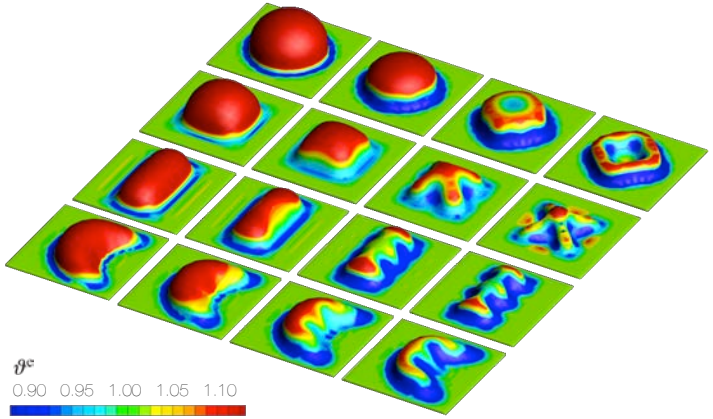

tissue expander deflation. spatio-temporal evolution of elastic area stretch. as the expander pressure is gradually removed, from left to right, the grown skin layer collapses. deviations from a flat surface after total unloading, right, demonstrate the irreversibility of the growth process.

example - skin expansion 50

residual stress - isotropic skin model

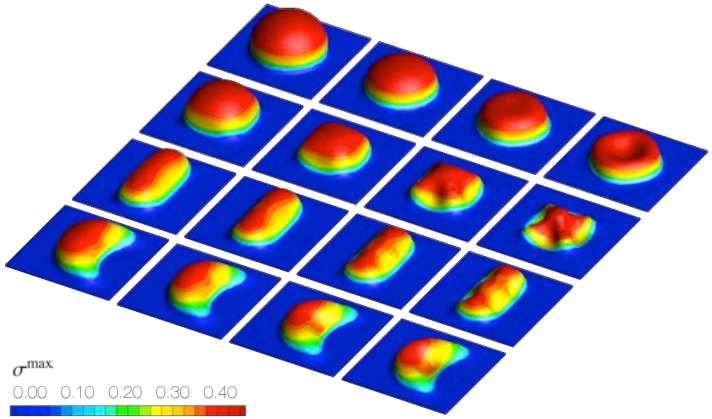

tissue expander deflation. spatio-temporal evolution of maximum principal stress. as the expander pressure is gradually removed, from left to right, the grown skin layer collapses. remaining stresses at in the unloaded state, right, are growth-induced residual stresses.

example - skin expansion 51

tissue expansion in pediatric forehead reconstruction

resurfacing of large congenital defects. the patient, a one-year old girl, presented with a giant congenital nevus. three forehead and scalp expanders were implanted simultaneously for in situ forehead flap growth. the follow-up photograph shows the girl at age three the initial defect was excised and resurfaced with expanded forehead and scalp flaps.

example - tissue expansion 52

tissue expansion in pediatric forehead reconstruction

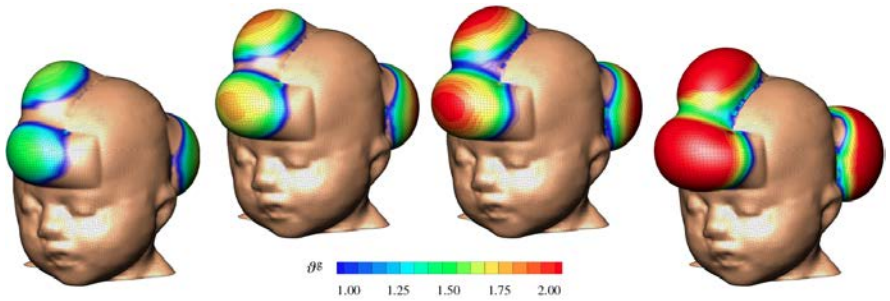

skin expansion in pediatric forehead reconstruction. case study I: simultaneous forehead, anterior and posterior scalp expansion.spatio-temporal evolution of area growth displayed at t=0.24, t=0.33, t=0.42 and t=0.75. the initial area of 149.4cm^2 increases gradually as the grown skin area increases to 190.2cm^2, 207.4cm^2, 220.4cm^2, and finally 251.2cm^2, from left to right.

example - tissue expansion 53

tissue expansion in pediatric forehead reconstruction

resurfacing of large congenital defects. the patient, a one-year boy, presented with a giant congenital nevus. simultaneous forehead, cheek, and scalp expanders were implanted for in situ skin growth. this technique allows to resurface large anatomical areas with skin of similar color, quality, and texture. the follow-up photograph shows the boy at age three after forehead reconstruction.

example - tissue expansion 54

tissue expansion in pediatric forehead reconstruction

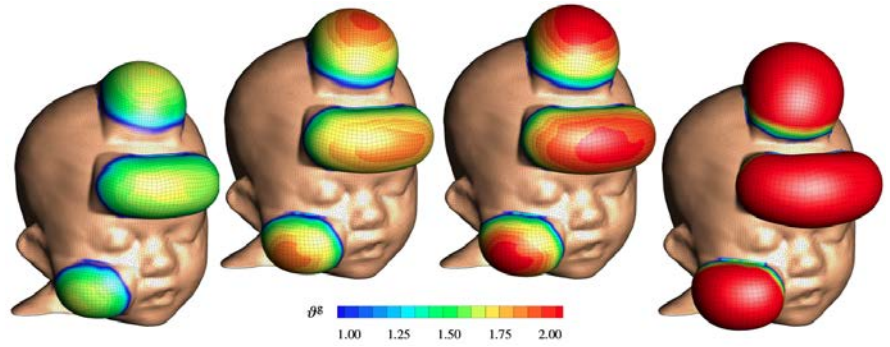

skin expansion in pediatric forehead reconstruction. case study II: simultaneous forehead, scalp, and cheek expansion.spatio-temporal evolution of area growth displayed at t=0.24, t=0.33, t=0.42 and t=0.75.the initial area of 128.7cm^2 increases gradually as the grown skin area increases to 176.0 cm^2,191.3 cm^2, 202.1 cm^2, and finally 227.1 cm^2, from left to right.

example - tissue expansion 55

tissue expansion in pediatric forehead reconstruction

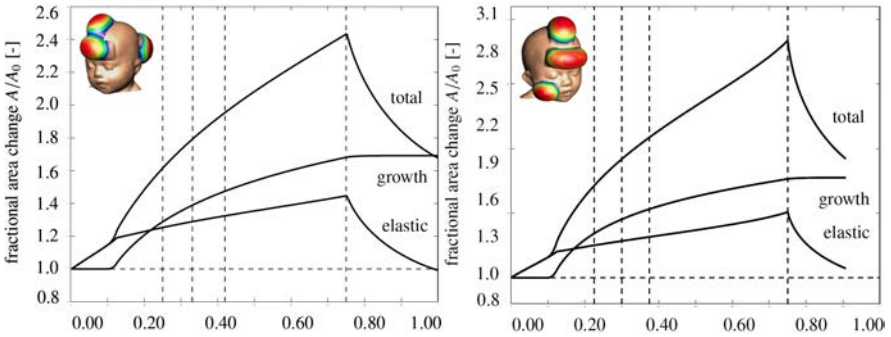

skin expansion in pediatric forehead reconstruction. case study I: simultaneous forehead, anterior and posterior scalp expansion, right. case study II: simultaneous forehead, scalp, and cheek expansion, left. vertical dashed lines correspond to the time points displayed in the previous figures.

example - tissue expansion 56